

Contagion Effect Estimation Using Proximal Embeddings

Zahra Fatemi

zfatem2@uic.edu

Department of Computer Science

University of Illinois Chicago

Elena Zheleva

ezheleva@uic.edu

Department of Computer Science

University of Illinois Chicago

ABSTRACT

Contagion effect refers to the causal effect of peers' behavior on the outcome of an individual in social networks. While prominent methods for estimating contagion effects in observational studies often assume that there are no unmeasured confounders, contagion can be confounded due to latent homophily: nodes in a homophilous network tend to have ties to peers with similar attributes and can behave similarly without influencing one another. One way to account for latent homophily is by considering proxies for the unobserved confounders. However, in the presence of high-dimensional proxies, proxy-based methods can lead to substantially biased estimation of contagion effects, as we demonstrate in this paper. To tackle this issue, we introduce the novel *Proximal Embeddings (ProEmb)*, a framework which integrates Variational Autoencoders (VAEs) and adversarial networks to generate balanced low-dimensional representations of high-dimensional proxies for different treatment groups and identifies contagion effects in the presence of unobserved network confounders. We empirically show that our method significantly increases the accuracy of contagion effect estimation in observational network data compared to state-of-the-art methods.

1 INTRODUCTION

Causal inference is central to data-driven decision-making. The goal of causal inference is to estimate the effect of an intervention on individuals' outcomes. Traditionally, causal inference has relied on the assumption of no interference, the assumption that any individual's response to treatment depends only on their own treatment and not on the treatment of others. However, individuals can impact each other through their interactions and by sharing their ideas and opinions. Contagion is a type of interference that is defined as the influence of neighbors' actions on an individual's actions. Contagion effect estimation plays a central role in understanding how social environments shape personal actions, behavior, and attitudes [7, 18, 21, 22]. Some real-world applications of contagion effect estimation include studying the spread of obesity from one person to another [9, 36], analyzing the spread of smoking behavior and decisions to quit among peers [10], understanding and quantifying the role of one's social environment in trusting fake news on online social media platforms [65, 67], and assessing the influence of peers on educational outcomes in online learning systems [40].

Despite their importance, identification (i.e. determining causal estimands based on observational data distribution [52]) and estimation of contagion effects are challenging due to the presence of unmeasured confounders, variables that affect both the treatment and the outcome of interest. The presence of unmeasured confounders breaks the strong ignorability assumption of causal inference [59, 60], the assumption that the treatment assignment of nodes is independent of potential outcomes conditioning on the observable variables, which

makes the causal effect unidentifiable. A common source of confounding in networks is latent homophily [46, 50, 63, 69]. Latent homophily is defined as the tendency of ties to form between individuals with similar unobserved attributes. When contagion effects are confounded with latent homophily, it is hard to tell if any changes in the individual's outcome are the result of neighbors' influence or the similarity between the individual and neighbors characteristics. For example, people with similar political affiliations would be more likely to interact on social media (e.g., Twitter) and they may express similar opinions (e.g., agree or disagree with social distancing policies during a pandemic), not because one influences the other but because they share similar political views in the first place.

To identify and estimate contagion effects in the presence of unobserved confounders, existing approaches look for observed variables that can be considered as valid proxies of the unobserved confounders [19, 48, 66]. However, such approaches can perform poorly on real-world observational data, such as web and social media, in which a high-dimensional covariate space is the norm. High-dimensional control proxies (e.g., tweet words of a user) lead to a sparse vector of model parameters and higher asymptotic bias and variance of the estimation [14]. Similarly, selection bias can also introduce variance when analyzing causal effects [3, 25, 33, 61]. Selection bias occurs when there is a mismatch in attribute distributions between the treatment and control groups. For instance, if the treatment group comprises mostly of individuals who prioritize their health and have friends who follow social distancing guidelines, while the control group comprises individuals who do not prioritize their health and have friends who largely disregard social distancing measures, comparing these two groups may yield unreliable estimates of contagion effects. A common method for dealing with selection bias in observational studies is matching, where a balanced sample is created by identifying similar units from the opposite treatment group. However, matching tends to encounter scalability issues when applied to high-dimensional data [1, 3].

Present Work. To address high-dimensionality and selection bias in real-world contagion estimation settings, we introduce *Proximal Embeddings (ProEmb)*, a framework for inferring contagion effects in homophilous networks. ProEmb learns embeddings that reflect the unobserved confounders using high-dimensional proxies in the observational data. Our framework consists of three main components: 1) an embedding learning component which maps high-dimensional proxies to low-dimensional latent representations, 2) a representation balancing component that addresses representation mismatch between treatment and control groups in the learned latent space, and 3) a counterfactual learning component, where an outcome model is trained to infer the potential outcomes of nodes based on the treatment and the low-dimensional representation of proxies. The primary goal of dimensionality reduction is to reduce bias and variance in the estimation by decreasing sparsity and the number

of model parameters that need to be estimated. We combine *Variational Autoencoders (VAEs)* and adversarial networks [23, 47] to map high-dimensional proxies to a probability distribution over the latent space with the goal of obtaining a balanced low-dimensional proxy representation for treatment and control nodes. To the best of our knowledge, this work is the first that integrates VAEs and adversarial networks to improve contagion effect estimation in networks with unobserved confounders. While the idea of using proxies for estimating contagion effects is not new [19], making this idea practical for high-dimensional applications suffering from selection bias is novel.

Key idea and highlights. To summarize, this paper makes the following main contributions:

- We formulate the problem of contagion effect estimation in networks when latent homophily and high-dimensional proxies of latent confounders are present.
- We propose a novel framework, ProEmb, that integrates VAEs, adversarial networks, and meta-learners to infer contagion effects in networks with latent homophily and high-dimensional proxies.
- Through empirical analysis, we demonstrate that existing methods for inferring contagion effects using high-dimensional proxies are prone to substantial bias and variance, while our proposed approach exhibits remarkable performance improvements over state-of-the-art techniques.

2 RELATED WORK

There is extensive research on interference, and contagion effect mitigation in randomized experiments [17, 18, 26, 68, 70]. However, less attention has been paid to contagion effect estimation [73]. Here, we review prior studies that focus on estimating causal inference in observational network data.

Contagion effect estimation in networks. Graphical models provide a way to represent interdependency between the variables in causal inference studies. Ogburn and VanderWeele [51] study the role of causal models in causal effect estimation in the presence of different types of interference. Shalizi and Thomas [63] by presenting different causal models show that in networks formed by latent homophily, contagion, and homophily can be confounded and the causal effect is not always identifiable. A more recent study shows that controlling for the cluster assignment of nodes in a homophilous network is sufficient to make contagion effects identifiable [62].

Causal inference using proxy variables. There is growing literature on causal inference with hidden confounders and observed proxies [15, 48, 49, 66]. However, less attention has been paid to proxies for contagion effect estimation. A recent study deploys negative control outcome and exposure variables to estimate contagion effects in low-dimensional space [19]. Our work builds upon this work and focuses on estimating contagion effects in datasets with high-dimensional proxies.

Causal inference using embeddings. Recently, a series of methods have been proposed to leverage representation learning to relax the strong ignorability assumption in networked data. Guo et al. [25] propose the Network Deconfounder framework where network structure and the observed features of nodes are mapped to a latent representation space to capture the influence of hidden confounders

and learn individual treatment effects from observational network data. Veitch et al. [71] propose a procedure for estimating treatment effects using network embeddings by reducing the causal estimation problem to a semi-supervised prediction of the treatments and outcomes and using embedding models for the semi-supervised prediction. Cristali and Veitch [12] use node embeddings learned from the network structure for estimating contagion effects in a different setting where covariates and the network structure are unobserved. This work presents a different approach from the method described in this paper.

Representation balancing. A line of research leverages weighting-based methods to balance covariates distribution [3, 13, 42, 43]. A different line of research combines weighting with representation learning to improve the distribution mismatch in causal effect estimation [25, 28, 44]. Shalit et al. [61] propose a data representation learning model that improves selection bias by fitting employing linear ridge regression and enforcing a relative error bound to address representation mismatch. Recently, Jiang and Sun [30] proposed the NetEst framework, which targets the representation learning for observed confounders. This approach integrates a discriminator component to tackle representation mismatch. It is worth mentioning that their methodology differs from ours in two key aspects. First, they assume that there are no unmeasured confounders, whereas our approach accounts for their presence. Second, they employ a distinct causal model that differs from the one presented in this paper.

3 PROBLEM STATEMENT

In this section, we present our data model, the causal estimand, different types of proxies, and issues with high dimensional proxies.

3.1 Data model

We assume a graph $G = (V, E)$ that consists of a set of $|V|$ nodes and a set of edges $E = \{e_{ij}\}$, where e_{ij} denotes that there is an edge between node $v_i \in V$ and node $v_j \in V$. Each node has an observed n -dimensional vector of attributes, Z_i , unobserved characteristics, U_i , and outcomes in two consecutive time steps, $Y_{i,t-1} \in \{0, 1\}$, and $Y_{i,t} \in \mathbb{R}$. If node v_i is activated at time $t - 1$ (e.g., obeyed social distancing policies), then $Y_{i,t-1} = 1$. Let $N_i = \{v_j | v_j \in V \ \& \ \exists e_{ij} \in E\}$ denote the set of neighbors of node v_i and A_i be the adjacency vector for node v_i where $A_{ij} = 1$ if $\exists e_{ij}$. For each node, there exists a set of neighbors' hidden characteristics U_{ngb} , a set of neighbors' observed attributes Z_{ngb} , and two sets of neighbors' outcomes $Y_{ngb,t-1}$ and $Y_{ngb,t}$. We further assume that edges form by latent homophily on U which means that nodes with more similar unobserved characteristics are more likely to connect [62].

3.2 Causal Model

Structural Causal Models (SCMs) are graphical representations of cause-effect relationships between variables that allow reasoning about identification of the effect of interest [52]. Causal Graphs are Directed Acyclic Graphs (DAGs) that represent SCMs, with variables as nodes and cause-effect relationships as edges. If variable Y is a child of variable X , we say that Y is caused by X , or that X is the direct cause of Y .

Following Egami and Tchetgen [19], we assume the causal graph depicted in Fig. 1, where the connections are formed based on

the similarity of the unobserved homophilous attributes. However, Egami and Tchetgen consider a chain graph [41] to represent network dependence of unobserved confounders across units. Hidden variables are represented by dashed circles.

In each connection, "ego" refers to a node whose contagion effects we estimate, and "peer" refers to a node that influences the ego's outcome. In this paper, treatment is the set of peer outcomes $Y_{ngb,t-1}$ and the outcome of interest is the ego's outcome $Y_{i,t}$. The potential outcome of node v_i under contagion effects is defined as the value that $Y_{i,t}$ would take if peer's outcome $Y_{ngb,t-1}$ had been set to y . The factual outcome $Y_{i,t}^F$ refers to the observed outcome of an individual when $Y_{ngb,t-1} = y$ and the counterfactual outcome $Y_{i,t}^{CF}$ shows the unobserved response of an individual when $Y_{ngb,t-1} = 1 - y$.

Given a set of activated neighbors $\tilde{N}_i \subseteq N_i$, we define $h : \{0, 1\}^{|\tilde{N}_i|} \rightarrow \{0, 1\}$ as a function over the neighbors' activations which maps the neighbors' activations to a binary value. In this paper, we consider the ego-networks connection model where multiple activated peers may exist ($|\tilde{N}_i| \geq 1$). Dyads, i.e., pairs of two individuals, are a special case of the ego-networks model where for every node v_i , $|\tilde{N}_i| = 1$ and an activated peer can activate an ego.

3.3 Contagion Effect Estimation

We define *Individual Contagion Effects (ICE)* as the difference between the outcome of node v_i under two different values for the neighbors' activation $h(Y_{ngb,t-1})$:

$$\tau_i = Y_{i,t}(h(Y_{ngb,t-1}) = 1) - Y_{i,t}(h(Y_{ngb,t-1}) = 0) \quad (1)$$

Our objective is to estimate ACE, which represents the average of ICE over all nodes and is measured as follows:

$$ACE(V) = \frac{1}{|V|} \sum_{i=1}^{|V|} \tau_i \quad (2)$$

In observational data, estimating ICE is challenging because we can never simultaneously observe the factual and counterfactual outcomes of a unit.

One of the main assumptions in inferring causal effects from observational data is strong ignorability or no unmeasured confounding. According to this condition, the potential outcomes of a node are independent of its treatment assignment given its observed attributes [59]. Under the strong ignorability assumption, adjusting for variables that block the back-door path allows for the identification of the causal effect [52]. A back-door path refers to a path from treatment to outcome in the structural causal model that has an arrow into the treatment variable. When unblocked back-door paths exist, there are two sources of association between treatment and outcome: one is causal (the causal effect of treatment on the outcome), and the other is non-causal (through the back-door path). In the presence of unblocked back-door paths, it becomes challenging to decide whether the observed association is a result of the causal effect or the spurious association enabled by the back-door path. In the causal model represented in Figure 1, strong ignorability holds if:

$$Y_{i,t}(1), Y_{i,t}(0) \perp\!\!\!\perp Y_{ngb,t-1} \mid Z_i, A_i \quad (3)$$

However, conditioning on A_i introduces a dependence association between unobserved variables U_i and U_{ngb} where the unblocked backdoor path $Y_{i,t} \leftarrow U_i \rightarrow A_i \leftarrow U_{ngb} \rightarrow Y_{ngb,t-1}$ violates

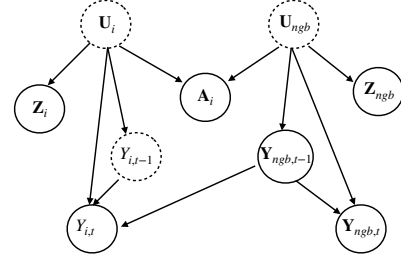


Figure 1: The causal model for the ego-network of ego v_i : Z_i and Z_{ngb} are proxies of the hidden confounders. U_i and U_{ngb} are unobserved homophilous attributes. Dashed circles show unobserved variables.

the ignorability assumption ($Y_{i,t} \not\perp\!\!\!\perp Y_{ngb,t-1} \mid A_i, Z_i$) and makes the contagion effects unidentifiable. We are interested in measuring ACE in the presence of an unobserved confounder, i.e., where the unobserved network confounder is the direct cause of the outcome of an ego and its peers. We assume the following common structural equations hold in our study:

$$Y_{i,t} = \theta h(Y_{ngb,t-1}) + \beta_u f(U_i) + \epsilon \quad (4)$$

$$Y_{ngb,t-1} = \gamma_u g(U_{ngb}) + \epsilon \quad (5)$$

where θ represents the causal effect we would like to infer. f and g can be any linear or non-linear functions.

3.4 Double Negative Control Proxies

One way to account for latent homophily is by considering proxies for unobserved confounders. Proxies are measurable variables that are correlated with the unobserved variable, and conditioning on them enables the identification of the causal effect [48]. Proxies can be classified into three types [66]: a) variables which are common causes of the treatment and outcome variables, b) potential causes of the treatment which is related to the outcome only through an unobserved common cause for which the variable is a proxy, and c) potential causes of the outcome which are related to the treatment only through an unobserved common cause for which the variable is a proxy.

Negative controls are two groups of common proxies that make the causal effect identifiable in settings with unobserved confounders: 1) *Negative Control Exposure (NCE)* is a treatment variable that does not causally affect the outcome of interest, and 2) *Negative Control Outcome (NCO)* is a variable that is not causally affected by the treatment of interest. NCE and NCO correspond to proxy types b and c, respectively. While there has been research on using negative controls to identify causal effects in i.i.d. data [39, 49, 64, 66], only recently Egami and Tchetgen [19] demonstrate that leveraging these two types of negative control proxies can enable the identification of contagion effects in networked data with unobserved confounders. In the causal model presented in Fig. 1, a variable Z_i is considered as an NCO if:

$$Z_i \perp\!\!\!\perp Y_{ngb,t-1} \mid U_i, U_{ngb}, A_i \quad (6)$$

and variable Z_{ngb} is considered as an NCE if:

$$Z_{ngb} \perp\!\!\!\perp Y_{i,t} | Y_{ngb,t-1}, U_i, U_{ngb}, A_i, \quad (7)$$

$$Z_{ngb} \perp\!\!\!\perp Z_i | Y_{ngb,t-1}, U_i, U_{ngb}, A_i. \quad (8)$$

Assumption 6 implies that the variable Z_i serves as an auxiliary variable that is independent of the treatment, given the unobserved confounders and the adjacency vector of the node. Assumptions 7 and 8 state that Z_{ngb} is an auxiliary variable that is conditionally independent of the node’s outcome at time t and the NCO variable, given the treatment, the unobserved confounders, and the adjacency vector of the node with respect to its neighbors. Auxiliary variables are variables that can help to make estimates on incomplete data, while they are not part of the main analysis [11].

After identifying the negative control proxies, various estimators can be employed to infer the causal effect of interest. One commonly used approach is the *Two-stage Least Squares estimator (TSLS)*. TSLS is a method commonly applied in linear models with instrumental variables, which are variables correlated with the predictor variable but uncorrelated with the outcome variable [2]. TSLS consists of two stages. In the first stage, a new variable is constructed using the instrumental variables. This variable serves as a proxy for the unobserved confounders. Then, in the second stage, the estimated values obtained from the first stage are utilized in place of the actual values of the unobserved confounders, and an *Ordinary Least Squares regression (OLS)* is performed to estimate the causal effect on the outcome of interest. OLS is a technique used for estimating the coefficients in linear regression models. Egami and Tchetgen [19] employ the TSLS estimator to quantify contagion effects by leveraging the NCE and NCO proxy variables as:

$$Y_{i,t} \sim Y_{ngb,t-1} + Z_i Z_{ngb} + Y_{ngb,t-1} \quad (9)$$

where the coefficient of $Y_{ngb,t-1}$ shows the estimated contagion effects.

3.5 Issues with high-dimensional proxies

Dimensionality refers to the number of attributes or features present in a dataset. High-dimensional datasets are characterized by a large number of attributes, such as bag-of-words vectors representing word occurrences in a document, customers’ extensive purchase history in recommender systems, or health data of patients. In the presence of high-dimensional data, the number of model parameters p exceeds the number of data samples n , a problem known as the “Large p Small n ” issue in causal effect estimation using regression models [5]. Estimating contagion effects using control proxies can be problematic when the NCO and NCE proxies are high-dimensional. In the presence of high-dimensional proxies, the matrix of model parameters becomes sparse and exhibits a low-rank structure [15]. A matrix is considered low-rank if the number of linearly independent variables is significantly smaller than the total number of variables. Including correlated variables in the estimation process increases the variance of the causal estimand [1, 14], which adversely affects the performance of the estimator [8, 27]. This issue becomes even more prominent in TSLS estimation, where the computational burden increases with the number of instruments or predictors.

The goal of this paper is to develop a method that can identify contagion effects in the presence of latent homophily and high-dimensional negative control proxies. More formally:

PROBLEM 1 (CONTAGION EFFECT ESTIMATION). *Let $G = (V, E)$ be a graph evolved by latent homophily with high-dimensional double negative control proxies, associated with nodes. Our goal is to find an estimate of the average contagion effect (ACE) $\hat{\theta}$ that minimizes the expected error between $\hat{\theta}$ and the true value of ACE θ .*

Next, we present our approach to tackle the contagion effect estimation problem.

4 PROXIMAL EMBEDDING FRAMEWORK FOR CONTAGION EFFECT ESTIMATION

To address high dimensionality and selection bias in contagion effect estimation, we introduce the *Proximal Embeddings (ProEmb)* framework. ProEmb has three main components, shown in Fig. 2. The first component deals with sparsity and high dimensionality by reducing the number of the initial dependent variables to a smaller number of uncorrelated variables [72]. One prominent method for dimensionality reduction is Variational Autoencoders (VAEs) [34, 57], which employ probabilistic models to learn low-dimensional representations capturing the underlying structure of the data [35]. Such methods combine highly correlated variables into a set of uncorrelated variables to reduce the variance and thereby enhance the optimality of the estimators [14].

However, simply applying VAEs to causal inference is not a good idea because embeddings generated by VAEs can vary across different treatment groups. To address this problem, the second component of ProEmb integrates adversarial networks to update the generated representation by VAEs and improve the distribution shift between the representation of treatment and control nodes proxies. This updated representation is then passed on to the third component which consists of a counterfactual learning module that measures counterfactual outcomes using meta-learners [38]. To the best of our knowledge, ProEmb is the first method that integrates VAEs, adversarial networks, and meta-learners to improve causal effect estimation more generally, and more specifically contagion effect estimation in networks with unobserved confounders. Next, we describe each component in more detail.

4.1 Embedding learning

The goal of this component is learning a low-dimensional representation of high-dimensional and sparse proxies while preserving the parts of proxies that are predictive of the outcomes. We assume that the experimenter has classified observed variables into NCO and NCE proxies based on assumptions 6-8. We use VAEs to learn low-dimensional representations for each node’s proxies, utilizing the attributes of the node and its neighboring nodes. VAEs are a type of autoencoder that represents inputs as probability distributions in the latent space and enforce regularization by ensuring that the distributions generated by the encoder closely resemble a standard Gaussian distribution. VAEs have demonstrated remarkable success in dimensionality reduction due to their ability to both capture the underlying structure of high-dimensional data and regularize the latent

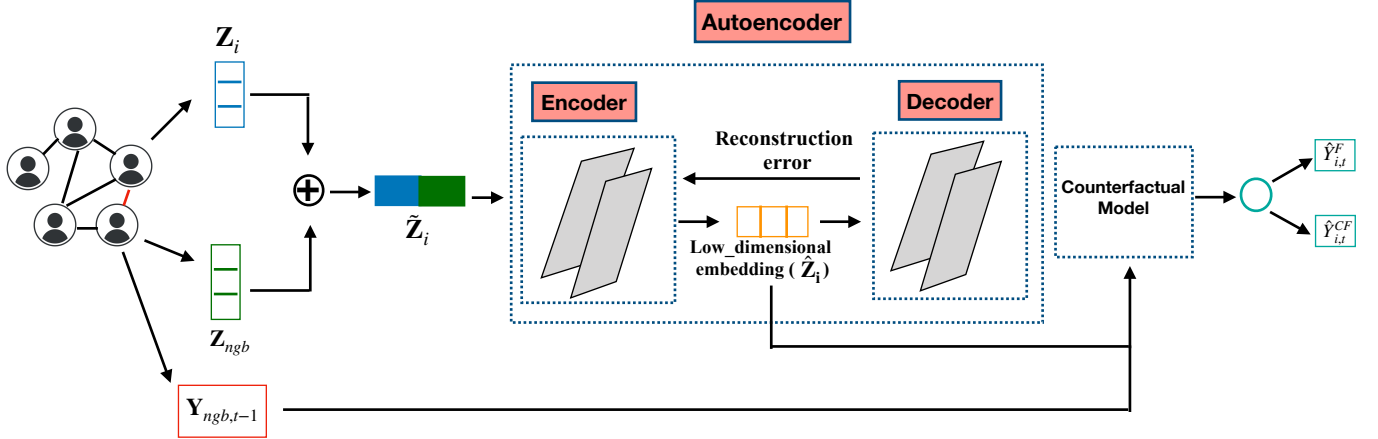


Figure 2: Illustration of the ProEmb framework with three components: 1) embedding learning where VAEs are used to generate low-dimensional embeddings of the proxies, 2) representation balancing where adversarial networks are used to improve the proxy representation mismatch between treatment and control nodes, and 3) counterfactual model where an estimator is trained to predict the counterfactual outcomes of treatment and control nodes.

space, which helps to prevent overfitting and improve generalization performance [24, 32, 55, 56].

In order to adapt VAEs to the problem of contagion estimation with high-dimensional proxies, one has to be careful to consider 1) how to capture latent homophily, 2) how to sample diverse low-dimensional representations from the representation space during training and inference, and 3) how to reconstruct the original high-dimensional proxy vectors, in order to evaluate and improve the performance of the model. ProEmb’s variational autoencoder addresses these considerations through each of its three parts:

- (1) *Probabilistic Encoder*. In order to infer the unobserved confounders, this component receives high-dimensional proxies as input and transforms them into a distribution in the latent space. Since Z_i as an NCO and Z_{ngb} as an NCE variable are proxies of the unobserved homophilous attributes, we expect to recover latent characteristics by applying a well trained encoder model to the concatenation of these proxies. Let $\tilde{Z}_i = \{z_{i,1}, \dots, z_{i,n}, z_{ngb,1}, \dots, z_{ngb,n}\}$ denote the concatenated vector of proxies $Z_i = \{z_{i,1}, \dots, z_{i,n}\}$ and $Z_{ngb} = \{z_{ngb,1}, \dots, z_{ngb,n}\}$ with dimension n . We use the encoder layer to map the proxies to the latent space with dimension m where $m < n$. The encoder uses L fully-connected layers to map \tilde{Z}_i to Z'_i , i.e.,

$$Z'_i = g(W_L \dots g(W_1 \tilde{Z}_i)) \quad (10)$$

where g indicates the activation function (e.g., Relu) and $\{W_l\}, l \in \{1, \dots, L\}$ represents the weight matrices of the fully connected layers of the encoder.

- (2) *Sampler*. In the VAEs framework, the sampler plays a crucial role in generating latent vectors from the learned distribution in the latent space. These latent vectors are randomly sampled from the distribution $p(\hat{Z}_i | \tilde{Z}_i)$, utilizing the mean and log-variance values obtained from the encoder’s output. The latent layer is represented by two sets of neurons: one

set representing the means of the latent space, and the other set representing the log-variances (which ensures positive variances). These values are measured as:

$$\mu = W_\mu Z'_i + \mathbf{b}^\mu \quad (11)$$

$$\ln \delta^2 = W_\delta Z'_i + \mathbf{b}^\delta \quad (12)$$

where \mathbf{b}^μ and \mathbf{b}^δ are vectors of biases. A proxy representation is sampled from the latent space as:

$$\hat{Z}_i \sim p(\hat{Z}_i | \tilde{Z}_i) = \mathcal{N}(\mu, \exp(\ln \delta^2)) \quad (13)$$

The output of the sampler, \hat{Z}_i , denotes the low-dimensional representation of the proxies which is later used by the counterfactual learning component for contagion effect estimation.

- (3) *Probabilistic Decoder*. The decoder takes the proxy representation \hat{Z}_i as input and tries to reconstruct the original proxy vector \tilde{Z}_i from it. The decoder uses \hat{L} fully-connected layers to map \hat{Z}_i to \tilde{Z}_i , i.e.,

$$Z''_i = f(\hat{W}_{\hat{L}} \dots f(\hat{W}_1 \hat{Z}_i)) \quad (14)$$

where Z''_i shows the reconstructed representation, f indicates the activation function, and $\{\hat{W}_l\}, l \in \{1, \dots, \hat{L}\}$ denotes the weight matrices of the fully connected layers of the decoder.

The objective of the VAEs component is to capture the relevant information from proxies while reducing the dimensionality. The loss function of VAEs consists of two main parts: 1) the reconstruction loss which measures the dissimilarity between the original input data and the data reconstructed by the VAEs, 2) the Kullback–Leibler (KL) divergence [37] which is a regularizer and quantifies the discrepancy between the inferred distribution $p(\hat{Z}_i | \tilde{Z}_i)$ and the known distribution $p(\tilde{Z}_i)$. The KL divergence encourages the latent space to

adhere to a prior distribution, typically a standard Gaussian distribution. The loss function of VAEs is defined as:

$$\mathcal{L}_{vae} = \frac{1}{|\mathcal{V}|} \sum_{i=1}^{|\mathcal{V}|} |z'_i - z_i|^2 + KL(p(\hat{\mathbf{Z}}_i|\tilde{\mathbf{Z}}_i)||p(\tilde{\mathbf{Z}}_i))_{i=1}^{|\mathcal{V}|}. \quad (15)$$

4.2 Representation balancing

Since the embedding learning models are trained on the factual outcomes and used to predict the counterfactual outcomes, minimizing the error in factual outcomes ($Y_{i,t}^F$) does not guarantee the simultaneous minimization of the error in counterfactual outcomes ($Y_{i,t}^{CF}$). Therefore, it is crucial to develop a model that addresses the mismatch between the distributions of treatment and control nodes in terms of their proxy representations. In this particular component, our focus is on enhancing proxy representation balancing to achieve similarity between the induced distributions for treated and control nodes. Inspired by [31], we employ the discriminator component of Generative Adversarial Networks (GAN) [23] to address the imbalance in the proxy representations generated by the VAEs for treatment and control nodes.

Let $\mathcal{D} : \hat{\mathbf{Z}}_i \rightarrow \{0, 1\}$ denote the discriminator function that maps the latent representation $\hat{\mathbf{Z}}_i$ to $Y_{i,t-1}$. Initially, we train the discriminator to maximize the probability of accurately predicting $Y_{i,t-1}$ from the latent representation $\hat{\mathbf{Z}}_i$. This is achieved by optimizing the following discriminator loss function:

$$\mathcal{L}_{\mathcal{D}} = \frac{1}{|\mathcal{V}|} \sum_{i=1}^{|\mathcal{V}|} (Y_{i,t-1} \log \mathcal{D}(\hat{\mathbf{Z}}_i) + (1 - Y_{i,t-1}) \log(1 - \mathcal{D}(\hat{\mathbf{Z}}_i))) \quad (16)$$

We update the latent representation $\hat{\mathbf{Z}}_i$ such that the distribution $p(Y_{i,t-1}|\hat{\mathbf{Z}}_i)$ becomes uniform. Considering that $Y_{ngb,t-1}$ is binary, a uniform distribution implies that $p(Y_{ngb,t-1} = 1|\hat{\mathbf{Z}}_i) = p(Y_{ngb,t-1} = 0|\hat{\mathbf{Z}}_i) = 0.5$. The $p(Y_{ngb,t-1}|\hat{\mathbf{Z}}_i)$ regularization loss is defined as:

$$\mathcal{L}_{rb} = \frac{1}{|\mathcal{V}|} \sum_{i=1}^{|\mathcal{V}|} (\mathcal{D}(\hat{\mathbf{Z}}_i) - 0.5)^2 \quad (17)$$

The regularization loss \mathcal{L}_{rb} is then backpropagated to the encoding part of the VAEs, enabling the update of the latent representation $\hat{\mathbf{Z}}_i$ such that the discriminator \mathcal{D} cannot accurately predict $Y_{ngb,t-1}$ from it. This ensures a more balanced and unbiased latent representation for treatment and control nodes' proxies.

4.3 Counterfactual learning

This component focuses on training a model to infer the counterfactual outcomes from low-dimensional embeddings of proxies $\hat{\mathbf{Z}}_i \in R^m$ as well as the peers' outcome $Y_{ngb,t-1}$. The factual outcomes are used to train the model. The objective function of this component during training is to minimize the error of the inferred factual outcomes defined as $\frac{1}{n} \sum_{i=1}^n (\hat{Y}_{i,t} - Y_{i,t})^2$ where $\hat{Y}_{i,t}$ indicates the predicted factual outcome by ProEmb.

Our framework can leverage advanced methods for estimating heterogeneous treatment effects that rely on machine learning techniques [4, 29, 33]. These methods are designed to estimate treatment effects in scenarios with heterogeneous treatment responses. We assume that the proxy representation is sufficiently informative

to satisfy the strong ignorability assumption ($Y_{i,t} \perp\!\!\!\perp Y_{ngb,t-1}|\hat{\mathbf{Z}}_i$), which allows us to make counterfactual predictions. To make this process more concrete, we demonstrate how our framework would use a common HTE estimation algorithm, the T-learner. However, our framework could leverage other HTE estimation algorithms as well. T-learner meta-learning algorithm is an example of such estimators and is used to measure Conditional Average Treatment Effect (CATE). A meta-learner is a framework to estimate the individual level causal effects using any supervised machine learning estimators (known as base-learners) [38]. The T-learner consists of two steps. First, two different base-learners are trained with treatment (μ_t) and control nodes (μ_c) to estimate the conditional expectations of the outcomes given observed attributes:

$$\mu_t(\mathbf{z}) = \mathbb{E}[Y_t(y=1)|\mathbf{Z}=\mathbf{z}] \quad (18)$$

$$\mu_c(\mathbf{z}) = \mathbb{E}[Y_t(y=0)|\mathbf{Z}=\mathbf{z}] \quad (19)$$

The treatment model is employed to predict the counterfactual outcomes of control nodes, and the control model is used to predict the counterfactual outcomes of treatment nodes. Then, the individual-level treatment effect is measured as:

$$\hat{\tau}(\mathbf{z}) = \hat{\mu}_t(\mathbf{z}) - \hat{\mu}_c(\mathbf{z}) \quad (20)$$

where $\hat{\mu}_t(\mathbf{z})$ and $\hat{\mu}_c(\mathbf{z})$ are learned estimates using treatment and control models. The T-learner has the advantage of being simple and flexible, as it utilizes any machine learning model as a base-learner.

5 EXPERIMENTS

In this section, we evaluate the performance of the ProEmb framework in contagion effect estimation compared to baselines.

5.1 Semi-synthetic data generation

As ground truth for causal effects is often unavailable in real-world datasets, researchers commonly rely on synthetic and semi-synthetic datasets to evaluate causal inference methods. In this section, we describe the semi-synthetic datasets we generated for our experiments. It is important to note that the generation doesn't consider embeddings and is therefore not biased towards an embedding-based solution. We utilize two real-world Twitter datasets: the *Hateful Users* dataset and the *Stay-at-Home (SAH)* dataset. In both datasets, we initially preprocess the data by removing URLs from tweet texts, converting all words to lowercase, and eliminating punctuation and stopwords. We also perform lemmatization and stemming on the words. Each tweet exhibits a unique distribution over several topics, reflecting the hidden semantic structure of the tweet. We consider the topic distribution of each tweet as the unobserved confounder U_i . To extract the topic distribution of each tweet, we employ Latent Dirichlet Allocation (LDA) [6] using the Python library *scikit-learn*. We utilize the elbow curve, which plots the number of topics against the coherence score, to determine the optimal number of topics. The coherence score evaluates the interpretability of topics by humans. **Hateful Users** dataset. This dataset is a sample of Twitter's retweet graph and consists of 100,386 users annotated as hateful or non-hateful, with 200 most recent tweets for each user [58]. In this dataset, we are interested in measuring the causal effect of users' hatefulness on the time their peers spend on the Twitter application/website. We randomly sample 5,000 tweets to create the final

Hateful Users dataset. and learn 50 LDA topics (selected based on coherence) to obtain the unobserved confounder vector. We extend this dataset by synthetically generating 1) connections representing user v_i retweeting user v_j 's tweet, 2) the outcome of each node at time $t - 1$, indicating the hatefulness of the user, and 3) the outcome of each node at time t , indicating the amount of time the individual spends on the Twitter application/website.

Stay-at-Home (SAH) dataset. This dataset comprises 206, 333 English tweets reflecting users' attitudes toward stay-at-home orders during the COVID-19 pandemic [20]. In our experiments, we randomly sample 30,000 tweets from this dataset and learn 20 LDA topics to capture the unobserved confounder vector. In this dataset, our objective is to investigate the causal effect of having friends who follow social distancing orders on the user's health. We augment the SAH dataset by synthetically generating: 1) connections indicating that user v_i retweeted user v_j 's tweets, 2) the outcome of each node at time $t - 1$, representing the stance of the tweet (whether it supports or opposes stay-at-home mandates), and 3) the outcome of each node at time t , indicating the level of user's health.

Ego-networks model. Since our causal model relies on the assumption that ties form between nodes by latent homophily, we generate the retweet networks synthetically. In this paper, we consider data on both networks and dyads and generate ties between nodes based on homophily. In the dyadic model, each node in the graph can only be connected to one other node. The probability of an edge forming between node v_i and v_j is determined by the cosine similarity of their latent attribute vectors \mathbf{U}_i and \mathbf{U}_j . In the network model, we follow [54] to generate networks growing based on homophily and preferential attachment. We start with $m_0 = 3$ fully connected seed nodes. At each time step, a new node v_j connects to $m = 3$ existing nodes, selected randomly with a probability $\pi(k_i|j)$ proportional to the node's degree k_i :

$$\pi(k_i|j) = \frac{\cos(\mathbf{U}_i, \mathbf{U}_j)k_i}{\sum_n \cos(\mathbf{U}_i, \mathbf{U}_n)k_n}. \quad (21)$$

In our network model, we assume that an activated neighbor v_j may activate an inactivated ego v_i with probability $p_j = 0.3$.

The advantage of considering both dyadic and network data is that it allows us to examine scenarios where a node is influenced by either a single activated neighbor or multiple activated neighbors. By considering dyadic data, we can focus on the interactions between pairs of nodes and gain insights into how one node's activation affects its immediate neighbor. This analysis provides valuable information about the dynamics at the micro-level. On the other hand, analyzing network data allows us to capture the broader influence of multiple activated neighbors on a node.

Counterfactual model. We generate the outcome of each node in two consecutive time steps. The outcome at time $t - 1$ is sampled as a binomial random variable with success probability that is a sigmoid function of \mathbf{U} :

$$Y_{i,t-1} = \text{Binom}(\text{sigmoid}(\alpha_u \mathbf{U}_i + \epsilon)) \quad (22)$$

where $\epsilon \sim \mathcal{N}(0, 1)$, and α_u is the unobserved confounder coefficient vector with the size of \mathbf{U}_j . We generate the factual and counterfactual

outcomes of each node at time t as:

$$Y_{i,t}^F = \beta_u \mathbf{U}_i + \beta_y Y_{i,t-1} + \tau h(Y_{ngb,t-1}) + \epsilon \quad (23)$$

$$Y_{i,t}^{CF} = \beta_u \mathbf{U}_i + \beta_y Y_{i,t-1} + \tau(1 - h(Y_{ngb,t-1})) + \epsilon \quad (24)$$

where β_u is the unobserved confounder coefficient vector with the size of \mathbf{U}_i . Among multiple peers that can activate an ego, one of them is selected to activate the node at the end which differs from the assumption made in [19] where the function h represents a mean aggregation function.

5.2 Experimental setup

In our experiments, we consider two types of attributes \mathbf{Z}_i . We use the bag-of-words (BoW) model to represent documents as vectors based on the occurrence of words within them. We utilize the *CountVectorizer()* function from the *Sklearn* library to obtain the BoW vectors. For both the SAH and Hateful Users datasets, this function generates BoW vectors with dimensions of 4,939 and 13,146, respectively. To understand the value of adding VAEs to our framework, we also experimented with simple embeddings derived from BoW. Word embeddings are numerical representations of words that capture semantic and syntactic information, as well as the contextual relationships between words in a document. We calculate the word embedding of each tweet by averaging the word embeddings of all tokens in the tweet. We employ two models to obtain the word embeddings. 1) Global Vectors for Word Representation (GloVe) is an unsupervised machine learning algorithm that maps words to a vector space, where the distances between word vectors reflect the semantic similarity between words [53]. We choose the GloVe-200d model trained on a dataset of 2B tweets, 27B tokens, and a vocabulary of 1.2M words. 2) Bidirectional Encoder Representations from Transformers (BERT) is a multi-layer bidirectional transformer encoder that maps a sequence of token embeddings and positional embeddings to the contextual representations of tokens [16]. We use the pre-trained BERT-base model containing 12 transformer layers, 12 attention heads in each layer, and 110M parameters in total. We refer to this model as *BERT*. We also further train the BERT model for 1,000 steps with each dataset to get new embeddings corresponding to the context of each dataset. We use the *AdamW* optimizer with a learning rate of $2e - 5$, max-seq-length of 128, and batch sizes of 32. We refer to this model as *BERT-ft*.

To understand the value of choosing different base-learners in our framework, we employ three types of base-learners for the T-Learner estimator: 1) Linear Regression (LR), 2) Gradient Boosted Trees (GB), and 3) Neural Network (NN), where two *Multi-layer Perceptrons (MLP)* are trained to predict the counterfactual outcomes of treatment and control nodes from the input features. In ProEmb with LR (PE-LR), ProEmb with GB (PE-GB), and ProEmb with NN (PE-NN) which are our proposed models, first, the integration of the VAEs and the discriminator is trained and applied to reduce the dimensionality of the proxies, and then T-Learner with different base-learners are deployed to predict the counterfactuals.

To train the VAEs, discriminators, and MLP models, we conduct a hyperparameter search for the learning rate and the number of epochs. The learning rate is searched within the set $\{0.1, 0.01, 0.001, 0.0001\}$, while the number of epochs is searched within $\{10, 30, 50, 70, 100\}$. The best results are achieved with a learning rate of 0.001 and 50

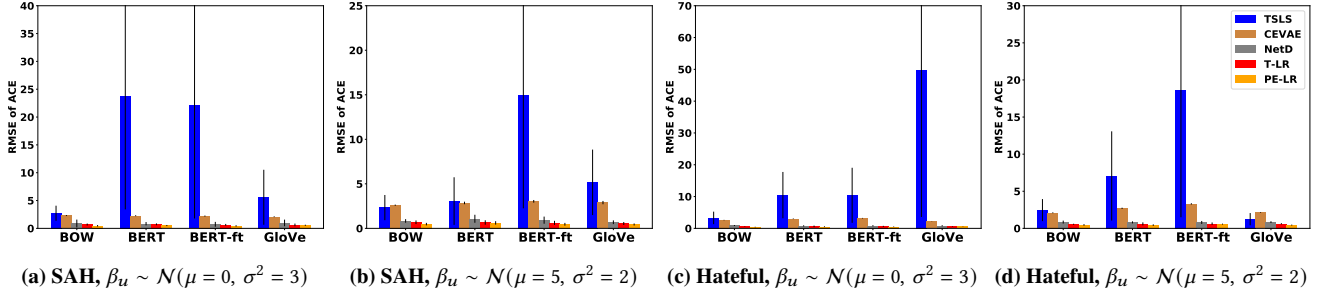


Figure 3: Comparison of RMSE of ACE using various baseline methods with network data. Error bars represent the standard deviation of the estimated effects. TSLS has significantly higher estimation bias and variance than PE-LR in all datasets.

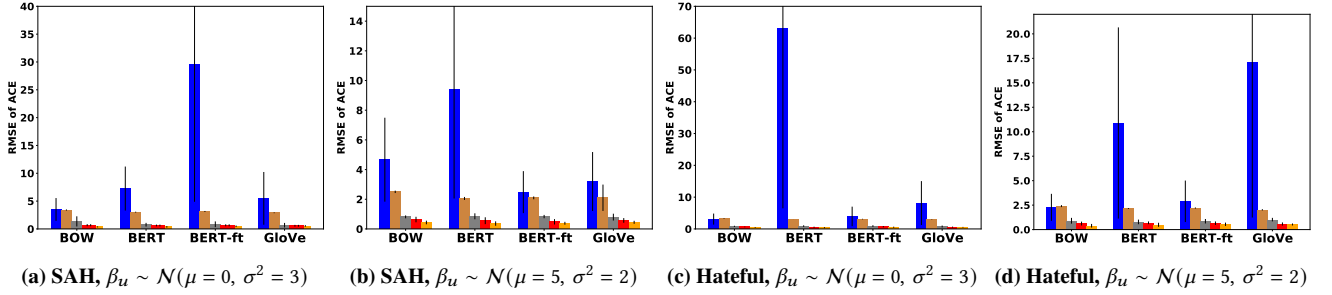


Figure 4: Comparison of RMSE of ACE using various baseline methods in dyadic data. Error bars represent the standard deviation of the estimated effects. TSLS has significantly higher estimation bias and variance than PE-LR in all datasets.

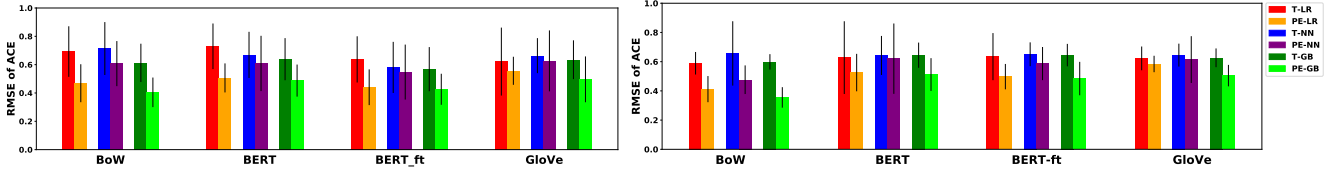


Figure 5: RMSE of ACE in SAH (left) and Hateful Users dataset (right) using network data and $\beta_u \sim N(\mu = 0, \sigma^2 = 3)$.

epochs for both models. For the VAEs, we search the number of hidden units of the hidden layers in $\{100, 200, 300\}$ and the number of encoder and decoder layers in 1, 2, 3, 4. We select a network with 100 hidden nodes, a 3-layer encoder, and a 3-layer decoder with a ReLU activation function. In the discriminator component, after hyperparameter search, we determine that four hidden layers, with linear activation functions, produce the best performance. The output layer utilizes a Sigmoid function. Regarding the MLP, we search for the number of hidden units and the number of fully connected layers. Ultimately, we train an MLP model with two fully connected layers, each containing 125 hidden units. We set the embedding dimension of the VAEs as the dimension of the unobserved confounder variable in each dataset (20 in SAH and 50 in the Hateful Users dataset).

To report the estimation error of different models, we measure the *Root Mean Squared Error (RMSE)* of contagion effects as:

$$RMSE = \sqrt{\frac{1}{S} \sum_{s=1}^S (\hat{ACE}_s - ACE_s)^2}$$

where S is the number of runs, ACE and \hat{ACE} are the true and estimated contagion effect in run s , respectively. In all experiments, we set S to 10 and τ_i to 1 for all nodes. We consider the BoW or word embedding vector of each user’s tweet as an NCO proxy and the BoW or word embedding vector of the peer’s tweet as an NCE proxy of the hidden topic distributions.

For generating factual and counterfactual outcomes using eq. 23-24, following [19], we set $\beta_y = 0.2$. In addition, we vary the strength of unobserved confounding coefficient vector β_u with two different distributions: $\beta_u \sim N(\mu = 5, \sigma^2 = 2)$ and $\beta_u \sim N(\mu = 0, \sigma^2 = 3)$. We also set $\alpha_u \sim N(\mu = 0, \sigma^2 = 1)$.

Baselines: We compare the performance of ProEmb variants against four different baselines:

- Two-stage Least-Squares estimator (TSLS) which is the only existing and state-of-the-art method that makes contagion effects identifiable in network data with unobserved confounders using negative control proxies [19]. We use *ivreg*

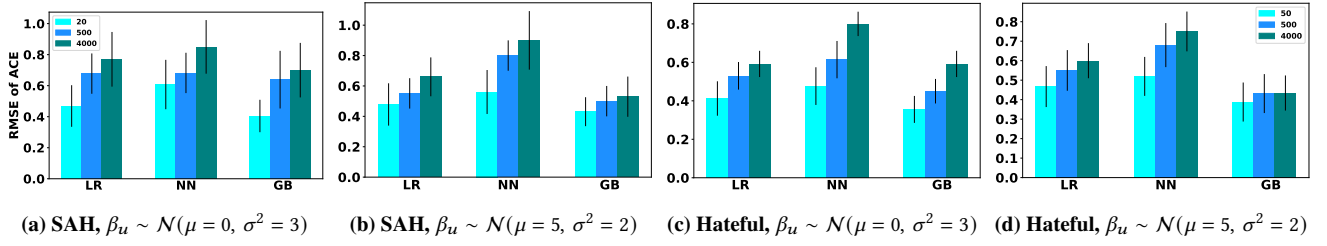


Figure 6: RMSE of ACE in ProEmb with varying embedding vector dimensions in SAH and Hateful Users dataset with network data. The x-axis represents different types of base-learners used in the counterfactual component of the ProEmb framework.

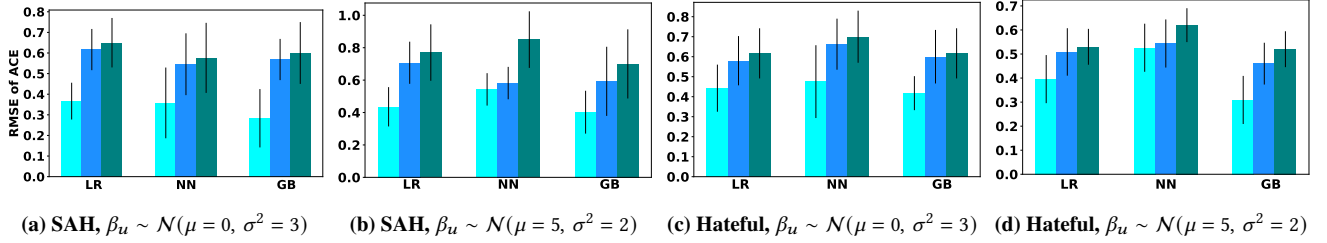


Figure 7: RMSE of ACE in ProEmb with varying embedding vector dimensions in SAH and Hateful Users dataset with dyadic data. The x-axis represents different types of base-learners used in the counterfactual component of the ProEmb framework.

function from R software to fit a TSLS estimator and infer the coefficient of $Y_{ngb,t-1}$ showing the contagion effects.

- *Causal Effect Variational Autoencoder (CEVAE)*: CEVAE is a VAEs-based model designed for inferring individual treatment effects (ITE) with unobserved confounders [45]. Although it is primarily intended for non-network datasets, it can be adapted to network data by concatenating available proxies for the unobserved confounders (Z_i and Z_{ngb}) as the noisy proxy vector for each node. We use the default hyperparameter settings of CEVAE in our experiments.
- *Network Deconfounder (NetD)*: NetD utilizes network information to infer latent confounders and estimate individual treatment effects [25]. It exploits Graph Convolutional Networks (GCNs) to learn representations of hidden confounders by simultaneously mapping features and network structure into a shared representation space. An output function is then learned to infer the potential outcome of a node based on the treatment and the representation of hidden confounders.
- We also consider only a T-Learner with Linear Regression (T-LR), Gradient Boosted Tree (T-GB), and neural network (T-NN) as the base-learners.

5.3 Results

5.3.1 Comparison to all baselines. In this experiment, we conduct an evaluation of different estimators to measure contagion effects. In Fig. 3, we present a comparison between all baselines (TSLS, CEVAE, NetD, and T-LR) and our method PE-LR in estimating ACE using various features as proxy variables in the SAH and Hateful Users datasets with network and dyadic data.

The results strongly indicate that in both datasets TSLS consistently achieves significantly higher error and variance compared to the other models, especially our proposed method PE-LR. This was one of the most surprising results in our study since TSLS is a well-established estimation method in causal inference. For instance, in the SAH dataset with $\beta_u \sim \mathcal{N}(\mu = 0, \sigma^2 = 3)$, we observe errors of 2.71 versus 0.46 with BoW, 23.73 vs. 0.50 with BERT, 22.07 vs. 0.44 with BERT-ft, and 5.58 vs. 0.55 with GloVe. Among the four baselines, the T-LR model significantly reduces estimation errors in both the network and dyadic data which is why we used T-Learner as a baseline in the next experiment.

5.3.2 Comparison between ProEmb variants. To assess the performance of variants of the ProEmb framework in reducing contagion effect estimation error, we compare the RMSE of estimated contagion effects using ProEmb and the best performing baseline, T-Learner, with different base-learners. As Fig. 5 shows, PE-LR and PE-GB outperform other methods in reducing ACE estimation error in both datasets. For example, PE-LR with BoW features obtains 33.3% and 30.8% estimation error reduction compared to T-LR in SAH with different β s. Results are consistent in the Hateful Users dataset. PE-LR with BoW features reduces the T-LR estimation error by 29.3% and 16.3% in graphs with $\beta_u \sim \mathcal{N}(\mu = 0, \sigma^2 = 3)$ and $\beta_u \sim \mathcal{N}(\mu = 5, \sigma^2 = 2)$, respectively. The RMSE for PE is consistently lower for different base-learners and different features even if they do not always appear to be statistically significant due to overlapping variance.

Due to space constraints, we omit the results showing the comparison between T-Learner and ProEmb variants with $\mathcal{N}(\mu = 5, \sigma^2 = 2)$ and dyadic data. These results are consistent with findings from datasets with network data. ProEmb variants achieve better contagion effect estimation compared to T-Learner variants. Results across

datasets show that PE-GB obtains better performance compared to other variants in most cases.

5.3.3 Sensitivity to the dimension of the embedding. To investigate the impact of the embedding vector dimension on the estimation error of ProEmb variants, we train the ProEmb models with BoW features and different numbers of embedding dimensions from (20 to 4000). Fig. 6 presents the performance of the ProEmb framework with various base-learners in the SAH and Hateful Users datasets using network data. We observe that ProEmb variants with a small number of dimensions, specifically 20 in the SAH dataset and 50 in the Hateful Users dataset, yield the lowest estimation error across both datasets. As the number of dimensions increases, the estimation error also increases for all ProEmb variants. For instance, in the SAH dataset, increasing the number of dimensions from 20 to 4,000 leads to an increase in the estimation error of the PE-GB variant from 0.4 to 0.7 for graphs with $\beta_u \sim \mathcal{N}(\mu = 3, \sigma^2 = 0)$, and from 0.43 to 0.52 for graphs with $\beta_u \sim \mathcal{N}(\mu = 5, \sigma^2 = 2)$. Similarly, in the Hateful Users dataset, increasing the number of dimensions from 50 to 4,000 results in an increase in the estimation error of the PE-LR variant from 0.41 to 0.59 for graphs with $\beta_u \sim \mathcal{N}(\mu = 0, \sigma^2 = 3)$, and from 0.46 to 0.6 for graphs with $\beta_u \sim \mathcal{N}(\mu = 5, \sigma^2 = 2)$. These results indicate that PE-GB with a dimension of 20 in the SAH dataset and 50 in the Hateful Users dataset achieves the lowest error among all ProEmb variants. Similar findings are observed when conducting experiments on dyadic data, as shown in Fig. 7.

6 CONCLUSION

In this paper, we introduce the Proximal Embeddings (ProEmb) framework for increasing the accuracy of contagion effect estimation in observational network data affected by latent homophily and selection bias. Our framework comprises three key components: 1) embedding learning, which utilizes Variational Autoencoders to map high-dimensional proxies to low-dimensional representations and capture latent homophily, 2) representation balancing, which leverages adversarial networks to address the representation mismatch between treatment groups' proxy representations, and 3) counterfactual learning, which employs meta-learners to estimate counterfactual outcomes. Our results demonstrate the superiority of the ProEmb framework compared to the baselines in reducing the contagion effect estimation error. We observe that using Bag-of-Words as the feature representation yields better results compared to word embedding methods. A potential future direction is developing a framework to account for multi-hop contagion effects in observational data with unobserved confounders.

REFERENCES

- [1] Alberto Abadie and Guido W Imbens. 2006. Large sample properties of matching estimators for average treatment effects. *econometrica* 74, 1 (2006), 235–267.
- [2] Joshua D Angrist and Guido W Imbens. 1995. Two-stage least squares estimation of average causal effects in models with variable treatment intensity. *Journal of the American statistical Association* 90, 430 (1995), 431–442.
- [3] Serge Assaad, Shuxi Zeng, Chenyang Tao, Shounak Datta, Nikhil Mehta, Ricardo Henao, Fan Li, and Lawrence Carin. 2021. Counterfactual representation learning with balancing weights. In *International Conference on Artificial Intelligence and Statistics*. PMLR, 1972–1980.
- [4] Susan Athey and Guido W Imbens. 2015. Machine learning methods for estimating heterogeneous causal effects. *stat* 1050, 5 (2015), 1–26.
- [5] JM Bernardo, MJ Bayarri, JO Berger, AP Dawid, D Heckerman, AFM Smith, and M West. 2003. Bayesian factor regression models in the “large p, small n” paradigm. *Bayesian statistics* 7 (2003), 733–742.
- [6] David M. Blei, Andrew Y. Ng, and Michael I. Jordan. 2003. Latent Dirichlet Allocation. *Journal of Machine Learning Research* 3, Jan (2003), 993–1022. <https://www.jmlr.org/papers/v3/blei03a>
- [7] Yann Bramoullé, Habiba Djebbari, and Bernard Fortin. 2009. Identification of peer effects through social networks. *Journal of econometrics* 150, 1 (2009), 41–55.
- [8] John C Chao and Norman R Swanson. 2005. Consistent estimation with a large number of weak instruments. *Econometrica* 73, 5 (2005), 1673–1692.
- [9] Nicholas A Christakis and James H Fowler. 2007. The spread of obesity in a large social network over 32 years. *New England journal of medicine* 357, 4 (2007), 370–379.
- [10] Nicholas A Christakis and James H Fowler. 2008. The collective dynamics of smoking in a large social network. *New England journal of medicine* 358, 21 (2008), 2249–2258.
- [11] Linda M Collins, Joseph L Schafer, and Chi-Ming Kam. 2001. A comparison of inclusive and restrictive strategies in modern missing data procedures. *Psychological methods* 6, 4 (2001), 330.
- [12] Irina Cristali and Victor Veitch. 2021. Using Embeddings to Estimate Peer Influence on Social Networks. In *NeurIPS 2021*.
- [13] Richard K Crump, V Joseph Hotz, Guido W Imbens, and Oscar A Mitnik. 2009. Dealing with limited overlap in estimation of average treatment effects. *Biometrika* 96, 1 (2009), 187–199.
- [14] Xavier De Luna, Ingeborg Waernbaum, and Thomas S Richardson. 2011. Covariate selection for the nonparametric estimation of an average treatment effect. *Biometrika* 98, 4 (2011), 861–875.
- [15] Ben Deaner. 2021. Many Proxy Controls. *arXiv preprint arXiv:2110.03973* (2021).
- [16] Jacob Devlin, Ming-Wei Chang, Kenton Lee, and Kristina Toutanova. 2019. BERT: Pre-training of Deep Bidirectional Transformers for Language Understanding. In *Proceedings of the 2019 Conference of the North American Chapter of the Association for Computational Linguistics: Human Language Technologies, Volume 1 (Long and Short Papers)*. ACL, Minneapolis, Minnesota, 4171–4186. <https://doi.org/10.18653/v1/N19-1423>
- [17] Dean Eckles, Brian Karrer, and Johan Ugander. 2017. Design and Analysis of Experiments in Networks: Reducing Bias from Interference. *Journal of Causal Inference* (04 2017).
- [18] D. Eckles, R. Kizilcec, and E. Bakshy. 2016. Estimating peer effects in networks with peer encouragement designs. *PNAS* (2016).
- [19] Naoki Egami and Eric J Tchetgen Tchetgen. 2021. Identification and Estimation of Causal Peer Effects Using Double Negative Controls for Unmeasured Network Confounding. *arXiv preprint arXiv:2109.01933* (2021).
- [20] Zahra Fatemi, Abhari Bhattacharya, Andrew Wentzel, Vipul Dhariwal, Lauren Levine, Andrew Rojecki, G Elisabeta Marai, Barbara Di Eugenio, and Elena Zheleva. 2022. Understanding Stay-at-home Attitudes through Framing Analysis of Tweets. *IEEE International Conference on Data Science and Advanced Analytics (DSAA)* (2022).
- [21] James H Fowler and Nicholas A Christakis. 2008. Estimating peer effects on health in social networks: a response to Cohen-Cole and Fletcher; Trogdon, Nonnemaker, Pais. *Journal of health economics* 27, 5 (2008), 1400.
- [22] Paul Goldsmith-Pinkham and Guido W. Imbens. 2013. Social Networks and the Identification of Peer Effects. *Journal of Business & Economic Statistics* 31, 3 (2013), 253–264. <https://doi.org/10.1080/07350015.2013.801251> [arXiv:https://doi.org/10.1080/07350015.2013.801251](https://doi.org/10.1080/07350015.2013.801251)
- [23] Ian Goodfellow, Jean Pouget-Abadie, Mehdi Mirza, Bing Xu, David Warde-Farley, Sherjil Ozair, Aaron Courville, and Yoshua Bengio. 2014. Generative Adversarial Nets. In *Advances in Neural Information Processing Systems*, Z. Ghahramani, M. Welling, C. Cortes, N. Lawrence, and K.Q. Weinberger (Eds.), Vol. 27. Curran Associates, Inc. https://proceedings.neurips.cc/paper_files/paper/2014/file/5ca3e9b122f61f8f06494e97b1afcc3-Paper.pdf
- [24] Karol Gregor, Ivo Danihelka, Alex Graves, Danilo Rezende, and Daan Wierstra. 2015. Draw: A recurrent neural network for image generation. In *International conference on machine learning*. PMLR, 1462–1471.
- [25] Ruo Cheng Guo, Jundong Li, and Huan Liu. 2020. Learning individual causal effects from networked observational data. In *WSDM*. 232–240.
- [26] M Elizabeth Halloran and Michael G Hudgens. 2012. Causal inference for vaccine effects on infectiousness. *The international journal of biostatistics* 8, 2 (2012), 1–40.
- [27] Christian Hansen, Jerry Hausman, and Whitney Newey. 2008. Estimation with many instrumental variables. *Journal of Business & Economic Statistics* 26, 4 (2008), 398–422.
- [28] Negar Hassanpour and Russell Greiner. 2019. Counterfactual Regression with Importance Sampling Weights. In *IJCAI*. 5880–5887.
- [29] Jennifer L Hill. 2011. Bayesian nonparametric modeling for causal inference. *Journal of Computational and Graphical Statistics* 20, 1 (2011), 217–240.
- [30] Song Jiang and Yizhou Sun. 2022. Estimating Causal Effects on Networked Observational Data via Representation Learning. In *Proceedings of the 31st ACM International Conference on Information & Knowledge Management*. 852–861.

- [31] Song Jiang and Yizhou Sun. 2022. Estimating Causal Effects on Networked Observational Data via Representation Learning. In *Proceedings of the 31st ACM International Conference on Information & Knowledge Management*. 852–861.
- [32] Danilo Jimenez Rezende, SM Eslami, Shakir Mohamed, Peter Battaglia, Max Jaderberg, and Nicolas Heess. 2016. Unsupervised learning of 3d structure from images. *Advances in neural information processing systems* 29 (2016).
- [33] Fredrik D. Johansson, Uri Shalit, and David Sontag. 2016. Learning Representations for Counterfactual Inference. In *ICML- Volume 48* (New York, NY, USA) (*ICML'16*). JMLR.org, 3020–3029.
- [34] Diederik P Kingma and Max Welling. 2014. Auto-Encoding Variational Bayes. *stat* 1050 (2014), 1.
- [35] Diederik P Kingma and Max Welling. 2014. Auto-encoding variational bayes. *International Conference on Learning Representations (ICLR)* (2014).
- [36] Brian V Krauth. 2005. Peer effects and selection effects on smoking among Canadian youth. *Canadian Journal of Economics/Revue canadienne d'économique* 38, 3 (2005), 735–757.
- [37] Solomon Kullback and Richard A Leibler. 1951. On information and sufficiency. *The annals of mathematical statistics* 22, 1 (1951), 79–86.
- [38] Sören R Künzel, Jasjeet S Sekhon, Peter J Bickel, and Bin Yu. 2019. Metalearners for estimating heterogeneous treatment effects using machine learning. *Proceedings of the national academy of sciences* 116, 10 (2019), 4156–4165.
- [39] Manabu Kuroki and Judea Pearl. 2014. Measurement bias and effect restoration in causal inference. *Biometrika* 101, 2 (2014), 423–437.
- [40] Chih-Hung Lai, Hung-Wei Lin, Rong-Mu Lin, and Pham Duc Tho. 2019. Effect of peer interaction among online learning community on learning engagement and achievement. *International Journal of Distance Education Technologies (IJDET)* 17, 1 (2019), 66–77.
- [41] Steffen L Lauritzen and Thomas S Richardson. 2002. Chain graph models and their causal interpretations. *Journal of the Royal Statistical Society: Series B (Statistical Methodology)* 64, 3 (2002), 321–348.
- [42] Fan Li, Kari Lock Morgan, and Alan M Zaslavsky. 2018. Balancing covariates via propensity score weighting. *J. Amer. Statist. Assoc.* 113, 521 (2018), 390–400.
- [43] Liang Li and Tom Greene. 2013. A weighting analogue to pair matching in propensity score analysis. *The international journal of biostatistics* 9, 2 (2013), 215–234.
- [44] Sheng Li and Yun Fu. 2017. Matching on balanced nonlinear representations for treatment effects estimation. *Advances in Neural Information Processing Systems* 30 (2017).
- [45] Christos Louizos, Uri Shalit, Joris M Mooij, David Sontag, Richard Zemel, and Max Welling. 2017. Causal effect inference with deep latent-variable models. *Advances in neural information processing systems* 30 (2017).
- [46] Charles F Manski. 1993. Identification of endogenous social effects: The reflection problem. *The review of economic studies* 60, 3 (1993), 531–542.
- [47] Lars Mescheder, Sebastian Nowozin, and Andreas Geiger. 2017. Adversarial variational bayes: Unifying variational autoencoders and generative adversarial networks. In *International conference on machine learning*. PMLR, 2391–2400.
- [48] Wang Miao, Zhi Geng, Eric J Tchetgen Tchetgen, et al. 2018. Identifying causal effects with proxy variables of an unmeasured confounder. *Biometrika* 105, 4 (2018), 987–993.
- [49] Wang Miao, Xu Shi, and Eric Tchetgen Tchetgen. 2018. A confounding bridge approach for double negative control inference on causal effects. *arXiv preprint arXiv:1808.04945* (2018).
- [50] Elizabeth L Ogburn, Oleg Sofrygin, Ivan Diaz, and Mark J Van Der Laan. 2017. Causal inference for social network data. *arXiv preprint arXiv:1705.08527* (2017).
- [51] Elizabeth L Ogburn and Tyler J VanderWeele. 2014. Causal diagrams for interference. *Statistical science* 29, 4 (2014), 559–578.
- [52] Judea Pearl. 2009. *Causality*. Cambridge Univ Press.
- [53] Jeffrey Pennington, Richard Socher, and Christopher D. Manning. 2014. GloVe: Global Vectors for Word Representation. In *EMNLP*. 1532–1543. <http://www.aclweb.org/anthology/D14-1162>
- [54] Gabriel G Piva, Fabiano L Ribeiro, and Angélica S Mata. 2021. Networks with growth and preferential attachment: modelling and applications. *Journal of Complex Networks* 9, 1 (2021), cnab008.
- [55] Stephen KN Portillo, John K Parejko, Jorge R Vergara, and Andrew J Connolly. 2020. Dimensionality reduction of SDSS spectra with variational autoencoders. *The Astronomical Journal* 160, 1 (2020), 45.
- [56] Yunchen Pu, Zhe Gan, Ricardo Henao, Xin Yuan, Chunyuan Li, Andrew Stevens, and Lawrence Carin. 2016. Variational autoencoder for deep learning of images, labels and captions. *Advances in neural information processing systems* 29 (2016).
- [57] Danilo Jimenez Rezende, Shakir Mohamed, and Daan Wierstra. 2014. Stochastic backpropagation and approximate inference in deep generative models. In *International conference on machine learning*. PMLR, 1278–1286.
- [58] Manoel Horta Ribeiro, Pedro H Calais, Yuri A Santos, Virgílio AF Almeida, and Wagner Meira Jr. 2018. Characterizing and detecting hateful users on twitter. In *ICWSM*.
- [59] Paul R Rosenbaum and Donald B Rubin. 1983. The central role of the propensity score in observational studies for causal effects. *Biometrika* 70, 1 (1983), 41–55.
- [60] Donald B Rubin. 1974. Estimating causal effects of treatments in randomized and nonrandomized studies. *Journal of educational Psychology* 66, 5 (1974), 688.
- [61] Uri Shalit, Fredrik D Johansson, and David Sontag. 2017. Estimating individual treatment effect: generalization bounds and algorithms. In *International Conference on Machine Learning*. PMLR, 3076–3085.
- [62] Cosma Rohilla Shalizi and Edward McFowland III. 2016. Estimating causal peer influence in homophilous social networks by inferring latent locations. *arXiv preprint arXiv:1607.06565* (2016).
- [63] Cosma Rohilla Shalizi and Andrew C Thomas. 2011. Homophily and contagion are generically confounded in observational social network studies. *Sociological methods & research* 40, 2 (2011), 211–239.
- [64] Rahul Singh. 2020. Kernel methods for unobserved confounding: Negative controls, proxies, and instruments. *arXiv preprint arXiv:2012.10315* (2020).
- [65] David Sterrett, Dan Malato, Jennifer Benz, Liz Kantor, Trevor Tompson, Tom Rosenstiel, Jeff Sonderman, and Kevin Loker. 2019. Who shared it?: Deciding what news to trust on social media. *Digital journalism* 7, 6 (2019), 783–801.
- [66] Eric J Tchetgen Tchetgen, Andrew Ying, Yifan Cui, Xu Shi, and Wang Miao. 2020. An introduction to proximal causal learning. *arXiv preprint arXiv:2009.10982* (2020).
- [67] Russell Torres, Natalie Gerhart, and Arash Negahban. 2018. Epistemology in the Era of Fake News: An Exploration of Information Verification Behaviors among Social Networking Site Users. *SIGMIS Database* 49, 3 (jul 2018), 78–97. <https://doi.org/10.1145/3242734.3242740>
- [68] J. Ugander, B. Karrer, L. Backstrom, and J. Kleinberg. 2013. Graph cluster randomization: Network exposure to multiple universes. In *KDD*.
- [69] Tyler J VanderWeele and Weihua An. 2013. Social networks and causal inference. *Handbook of causal analysis for social research* (2013), 353–374.
- [70] Tyler J VanderWeele, Eric J Tchetgen Tchetgen, and M Elizabeth Halloran. 2012. Components of the indirect effect in vaccine trials: identification of contagion and infectiousness effects. *Epidemiology (Cambridge, Mass.)* 23, 5 (2012), 751.
- [71] Victor Veitch, Yixin Wang, and David Blei. 2019. Using embeddings to correct for unobserved confounding in networks. *Neurips* 32 (2019).
- [72] Wei Wang, Yan Huang, Yizhou Wang, and Liang Wang. 2014. Generalized autoencoder: A neural network framework for dimensionality reduction. In *CVPR workshops*. 490–497.
- [73] Elena Zheleva and David Arbour. 2021. Causal inference from network data. In *Proceedings of the 27th ACM SIGKDD Conference on Knowledge Discovery & Data Mining*. 4096–4097.